JCTC Journal of Chemical Theory and Computation

Article

pubs.acs.org/JCTC

Predicting the Sensitivity of Multiscale Coarse-Grained Models to their Underlying Fine-Grained Model Parameters

Jacob W. Wagner,‡ James F. Dama,‡ and Gregory A. Voth*

Department of Chemistry, James Franck Institute, Institute for Biophysical Dynamics, and Computation Institute, University of Chicago, 5735 South Ellis Avenue, Chicago, Illinois 60637, United States

Supporting Information

ABSTRACT: The sensitivity of a coarse-grained (CG) force field to changes in the underlying fine-grained (FG) model from which it was derived provides modeling insight for improving transferability across interaction parameters, transferability across temperature, and the calculation of thermodynamic derivatives. Methods in the literature, such as multi-trajectory finite differences and reweighted finite differences, are either too computationally demanding to calculate within acceptable noise tolerances or are too biased for practical accuracy. This work presents a new reweighting-free, single-simulation formula that allows for practical, high signal-to-noise calculations of CG model sensitivity with respect to FG model interaction parameters and thermodynamic state points. This formula, the self-consistent basis (SCB) single point formula, determines the many-body sensitivity in a single step by approximating the derivative of the many-body potential projected onto the same set of trial functions as the sensitivity. A related diagnostic formula also derived in this paper is the self-consistent iterative (SCI) single point formula, which is useful for identifying the importance of many-body sources of error and verifying CG representability of observables. The SCI formula determines the many-body sensitivity iteratively via a series of partially self-consistent, variational approximations to the complete many-body sensitivity. The new, computationally efficient SCB formula shows substantially less noise than previous methods when applied to single site methanol and solvent-free sodium chloride CG models, though bias can remain a problem. It represents a novel method for calculating alchemical transferability across interaction parameters at low computational cost and with high fidelity, and the results point to new understanding of the current limits of CG model transferability.

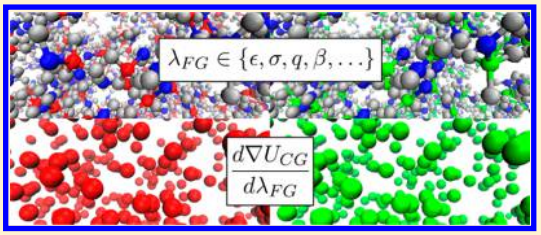

I. INTRODUCTION

Coarse-grained (CG) models seek to capture the essential details of fine-grained (FG) models at reduced computational cost by eliminating degrees of freedom (DOF).[1−4] To further increase computational savings with CG models, it is desirable to know when one can reuse the same CG model to describe FG models similar to the original FG model that was used to parametrize the CG model. Unfortunately, CG models tend to have limited transferability because eliminating DOF leads to state point-dependent effective interactions.[5,6] The dual problem to designing transferability is the determination of model sensitivity (i.e., how a CG model would change if it were parametrized under a different set of FG interactions or at a different state point). CG sensitivities can be used simply to determine the transferability of CG models, but a more promising and enterprising approach is to correct CG models with the changes predicted from the calculated sensitivities. However, for this to be practical, one must have a method of calculating sensitivities that is more computationally cost-effective than running new FG simulations to directly calculate new CG interactions at each new state point. In this article, we address this need for a computationally efficient method to calculate model sensitivities by proposing novel formulas for computationally efficient, low noise estimates of sensitivities from single FG simulations.

The model sensitivity of molecular systems has been extensively investigated at a single, all-atom (AA) level of resolution. Wong and Rabitz[7,8] calculated changes in free energy as a function of changes in the input Lennard-Jones (LJ) parameters in the simplest, linear response sense of sensitivity using a finite difference (FD). Using ad hoc modifications to FDs, Rocklin et al.[9] calculated the sensitivities of binding free energies to changes in interaction parameters. More computationally efficient methods employing single state and multistate statistical reweighting[10−12] can also be used to obtain estimates of the sensitivity using FDs and have been used to determine potential sensitivity to interaction cutoffs.[13] Fleishman and Brooks took a different approach,[14] using derivatives of the partition function and thermodynamic integration to calculate sensitivity of entropy and enthalpy via perturbation theory. Later, Wong, Thacher, and Rabitz used careful statistical mechanical derivations to determine first and second order sensitivity coefficients.[15] These sensitivity coefficients have been used in materials designed to optimize binding free energies by changing cation interactions[16] and to determine which input parameters are most influential in determining observables.[17] Recently, an expanded set of sensitivity equations

Received: February 24, 2015
Published: June 25, 2015

DOI: 10.1021/acs.jctc.5b00180
J. Chem. Theory Comput. 2015, 11, 3547−3560

were applied to improve a classical water model's agreement with ab initio and experimental measures.[18] However, sensitivities calculated at a single level of resolution do not address the problem of CG model transferability.

Sensitivity between models of two different resolution levels has been the subject of limited study. Krishna et al.[19] used the multiscale coarse-graining (MS-CG) methodology[20−23] and statistical reweighting over temperatures to get different CG potentials, which is a complementary approach to the one taken in this paper. Lu et al.[24] used FDs with MS-CG to decompose free energies into entropic and enthalpic components using sensitivity to temperature. As an alternative, some researchers have tried to increase the transferability of CG potentials by including extra independent variables. A few of these approaches included three-body interactions,[25,26] temperature-dependent terms,[27,28] density-dependent terms,[29−31] and concentration-dependent terms.[32] However, although much work has been done to improve the transferability of CG potentials, only reweighting and FD approaches have been used to probe sensitivity in multiscale calculations.

Several systematic approaches for developing CG models could potentially be used as a starting point for developing methods to calculate sensitivities, including relative entropy (RE),[33] inverse Monte Carlo (IMC),[34] iterative Boltzmann inversion (IBI),[35] force matching (FM),[20−23,36,37] and the generalized Yvon−Born−Green (g-YBG) equations.[38,39] RE minimization is a general approach in which one aims to minimize the loss of Shannon information from the FG model to the CG model potential.[33] If RE is minimized using Newton's method,[34] one obtains IMC,[40] which inverts radial distribution functions (RDF) iteratively to provide interaction potentials—though sampling noise must be taken into account.[41] Similarly, IBI inverts the RDF iteratively and is an approximate RE minimization, just as IMC is, using a fixed-point optimization that is simpler than that of Newton's method.[42] Likewise, FM and g-YBG, implemented as MS-CG, converge to the same result as RE in the limit of a complete basis set because FM minimizes the average of the gradient squared of the relative entropy.[43] Because RE converges to the same results as IBI, IMC, FM, and g-YBG in the appropriate limits,[42] it is important to consider which method is most appropriate given the limitations of the problem at hand. In the case that sampling is incomplete at short interaction distances and there are potential issues with basis sets to describe both the CG potential force field and the sensitivity of the CG potential or force field, the local nature of MS-CG becomes appealing. Local nature here refers to the fact that, in MS-CG, the fit in each portion of the force field is linked linearly to fits in other portions through a g-YBG equation[38,39] rather than through a complex, nonlinear, and nonlocal dependence. This feature of MS-CG removes the nonlinearity found in the other global, distribution-matching minimization methods, thus leading to a more direct, computationally straightforward method of calculating sensitivity better suited to rapid prototyping.

The present work develops reweighting-free, single simulation formulas that calculate the sensitivity of CG potentials and force fields to changes in the underlying FG interaction parameters and state points at the level of linear response. The calculated sensitivities are used to develop corrections to CG models that increase model accuracy when the CG potentials and force fields are transferred alchemically across interaction parameters or thermodynamically across state points. The accuracy of these predicted sensitivities are evaluated by comparison with reweighted FDs, and the accuracy of the corrected, transferred potentials are compared against potentials without any sensitivity correction. The remainder of the article is structured as follows: Sec. II describes the derivation and significance of the formulas developed in this work as well as the numerical and simulation methods used. Sec. III shows the application of these formulas to single site methanol and solvent-free sodium chloride systems and the resulting accuracy of the predicted sensitivities and potentials and then provides a general discussion of those results, including suggestions for future work. Sec. IV provides conclusions.

II. THEORY AND METHODS

A. Sensitivity Theory. The fundamental measure of sensitivity to small changes is the derivative

$$\frac{\mathrm{d}U(\mathbf{R}^N;\lambda)}{\mathrm{d}\lambda} = \lim_{\delta\lambda \to 0} \frac{U(\mathbf{R}^N;\lambda+\delta\lambda) - U(\mathbf{R}^N;\lambda-\delta\lambda)}{2\delta\lambda} \tag{1}$$

Here, the sensitivity of the CG potential $U(\mathbf{R}^N;\lambda)$ to a FG parameter λ is calculated by finding the difference between CG potentials obtained using modified FG parameters $\lambda \pm \delta\lambda$. In the above equation, $\mathbf{R}^N$ are the CG configurational variables. This method requires the calculation of at least two CG potentials to calculate the sensitivity. However, the range of $\delta\lambda$ in which this limit is approached, known as the linear regime, is not known a priori. This means that in fact more than two CG potentials must be calculated to verify the meaningfulness of a single calculated sensitivity. A second problem with this FD approach is that the random noise and fluctuations in estimates of the CG potentials are magnified dramatically when $\delta\lambda$ is small, exactly where the limit is approached. For the FD approach to be feasible, therefore, one must find a $\delta\lambda$ that is both in the linear regime and sufficiently large to make pulling the sensitivity signal out of sampling noise tractable, but there is no guarantee that such a $\delta\lambda$ exists in every case.

An alternative to the basic multitrajectory FD (MTFD) is to use statistical reweighting to obtain the CG potentials at different $\delta\lambda$ values from a single FG simulation. Statistical reweighting reuses configurations generated using a given parametrization by applying a reweighting factor, the ratio between Boltzmann factors across parametrizations, to the results of reanalyzing the configurations using a different parametrization. For generating CG models using MS-CG or g-YBG, this amounts to weighting the FM residual from the reevaluated forces by the exponential of the difference in the CG potential calculation (or inverse temperature, if temperature is varied). The use of a single trajectory in reweighting should minimize the noise seen at small $\delta\lambda$, which makes this approach appear relatively promising compared to FD, but the range of the linear regime is still not known a priori. Another problematic condition required for reweighting to be practical is that the original ensemble and the ensemble estimated by reweighting must have significant overlap so that the reweighted trajectory can give reliable averages. Furthermore, the averages are susceptible to bias when the original sample may not provide configurations that overlap with the reweighted ensemble evenly. An example of this is the application of reweighting to calculate averages at higher temperatures than the temperature of an initial simulation. Because the original trajectory explores only a subvolume of the

DOI: 10.1021/acs.jctc.5b00180
J. Chem. Theory Comput. 2015, 11, 3547−3560

phase space explored at higher temperatures, the reweighting procedure typically biases the resulting potentials to over-represent behavior characteristic of lower-energy conformations. For reweighting across interaction parameters, it is not always clear when this is a problem or how significant the bias may be—even after the calculation is complete.

Ideally, one would like a method of calculating sensitivities in the linear regime that does not depend on knowledge of the size of the linear regime, requires minimal computation, and is less susceptible to bias than a reweighted finite difference (RFD). We can do so by analytically evaluating the limit in the FD above, then using the resulting formulas to make our calculations. Starting from the FD formula above, one arrives at the equation

$$\frac{\mathrm{d}U_{\mathrm{CG}}(\mathbf{R}^N;\,\lambda)}{\mathrm{d}\lambda} = \left\langle \frac{\mathrm{d}u(\mathbf{r}^n;\,\lambda)}{\mathrm{d}\lambda} \right\rangle_{\mathbf{R}^N,\lambda} \tag{2}$$

where $u(\mathbf{r}^n;\lambda)$ is the FG potential in terms of the FG coordinates $\mathbf{r}^n$. However, this equation is remarkably data-inefficient: it only uses one scalar value of information per sampled frame, the derivative of the potential with respect to λ for that frame. Fitting a many-body function with many free parameters requires a great deal of input training data, and using only one datum per frame of input data would require a huge number of frames to properly parametrize the many-body sensitivity. Therefore, we apply a trick with a long history. By analogy to FM,[20,22,23,36,37,44] which uses more data per frame than potential matching by matching derivatives of the potential with respect to particle positions instead of matching per-frame potentials directly, one can also derive formulas for sensitivity matching that match the sensitivity of the derivatives of the potential with respect to all particle positions instead of matching the per-frame sensitivity directly. The gain in information per frame is proportional to the number of particles, which can be quite large. The remainder of this section describes the derivation of two such formulas, each of which results from a different approach to the problem of representing the many-body sensitivity in a reduced space of trial functions. *We propose that the first formula be used for practical calculation of sensitivity and the second formula be used as a theoretical diagnostic tool.*

Self-Consistent Basis (SCB) Single Point Formula. In the first derivation, we find a formula by considering the sensitivity of approximations to the many-body potential. After all, any practical CG potential will be an approximation, and we are therefore interested in the sensitivity of approximations when we talk about the sensitivity of CG models. A natural choice here is to look at the sensitivity of an approximate CG potential in the same set of trial functions used to construct the CG potential; because the basis functions for the CG potential and sensitivity are the same in this case, we call this a self-consistent basis (SCB) single point formula. To construct this formula, one needs to start from the FM residual expression reweighted from λ to $\lambda + \delta\lambda$ with the framewise weight function

$$w_t(\mathbf{r}^n;\,\lambda,\,\delta\lambda) = \frac{\exp(-\beta u(\mathbf{r}^n,\,\lambda+\delta\lambda) + \beta u(\mathbf{r}^n;\,\lambda))}{\frac{1}{N_t}\sum_{t=1}^{N_t}\exp(-\beta u(\mathbf{r}^n,\,\lambda+\delta\lambda) + \beta u(\mathbf{r}^n;\,\lambda))} \tag{3}$$

where N_t is the total number of simulation frames. Optimization of the residual with respect to basis functions to obtain the reweighted FM normal equations yields[23,45]

$$\frac{1}{N_t}\sum_{t=1}^{N_t} w_t(\mathbf{r}^n;\,\lambda,\,\delta\lambda)\mathbf{F}^T\mathbf{F}\phi = \frac{1}{N_t}\sum_{t=1}^{N_t} w_t(\mathbf{r}^n;\,\lambda,\,\delta\lambda)\mathbf{F}^T\mathbf{f} \tag{4}$$

where $\mathbf{F}$ is a matrix of configurational information about the basis function values for each particle, $\mathbf{f}$ is the 3N vector of the target forces, and ϕ is a vector of the unknown linear basis function coefficients. Then, taking a derivative of both sides with respect to $\delta\lambda$ and taking the limit $\delta\lambda \to 0$, a set of normal equations for the sensitivity emerges. Taking the limit of a long trajectory and a complete basis set and then rearranging those normal equations, the expression for the approximate sensitivity matching in terms of thermodynamic averages is

$$\begin{aligned}\frac{\mathrm{d}\nabla U(\mathbf{R}^N;\,\lambda)}{\mathrm{d}\lambda} = \Bigg\langle & M^{\dagger}\left(\frac{\mathrm{d}\nabla u(\mathbf{r}^n;\,\lambda)}{\mathrm{d}\lambda}\right) - \frac{\beta}{N_{\mathrm{CG}}}\Bigg(\frac{\mathrm{d}u(\mathbf{r}^n;\,\lambda)}{\mathrm{d}\lambda} \\ & - \left\langle \frac{\mathrm{d}u(\mathbf{r}^n;\,\lambda)}{\mathrm{d}\lambda} \right\rangle_{\lambda}\Bigg)(M^{\dagger}(\nabla u(\mathbf{r}^n;\,\lambda)) \\ & - \nabla U_{\mathrm{CG}}(\mathbf{R}^N;\,\lambda))\Bigg\rangle_{\mathbf{R}^N,\lambda}\end{aligned} \tag{5}$$

where $\langle \mathrm{d}u(\mathbf{r}^n;\lambda)/\mathrm{d}\lambda\rangle_{\lambda}$ is the Boltzmann weighted expectation value of $\mathrm{d}u(\mathbf{r}^n;\lambda)/\mathrm{d}\lambda$ over the entire FG ensemble, N_{CG} is the number of CG sites in order to make the sensitivity intensive, and $M^{\dagger}(...)$ is the mapping operator that transforms the FG forces into CG forces (see Appendix B for derivation and details). Every term on the right can be estimated directly from the simulation, so these estimates can be calculated in a single step without iteration.

Self-Consistent Iterative (SCI) Single Point Formula. An interesting alternative to the derivation in the previous section is to consider what the expression would be like if one treated the sensitivity of the many-body potential directly, regardless of basis set limitations. A sensitivity estimator based on approximating the sensitivity of a full basis set potential using a finite basis set rather than on the sensitivity of approximate potentials using finite basis sets would provide a diagnostic for assessing the importance of renormalized many-body effects in CG sensitivities. As before, we look for a formula in terms of derivatives of forces instead of derivatives of potentials. Starting from the FD of the forces with the averages in the $\lambda \pm \delta\lambda$ ensembles written explicitly, then substituting the mapped FG forces for the CG forces, the transformation of these ensembles to a common λ ensemble leads to

$$\begin{aligned}\frac{\mathrm{d}\nabla U(\mathbf{R}^N;\,\lambda)}{\mathrm{d}\lambda} = & \lim_{\delta\lambda\to 0}\frac{1}{2\delta\lambda} \\ & \Bigg\langle M^{\dagger}(\nabla u(\mathbf{r}^n;\,\lambda+\delta\lambda))\frac{e^{-\beta u(\mathbf{r}^n;\lambda)+\beta u(\mathbf{r}^n;\lambda+\delta\lambda)}}{\left\langle e^{-\beta u(\mathbf{r}^n;\lambda)+\beta u(\mathbf{r}^n;\lambda+\delta\lambda)}\right\rangle} \\ & - M^{\dagger}(\nabla u(\mathbf{r}^n;\,\lambda-\delta\lambda))\frac{e^{-\beta u(\mathbf{r}^n;\lambda)+\beta u(\mathbf{r}^n;\lambda-\delta\lambda)}}{\left\langle e^{-\beta u(\mathbf{r}^n;\lambda)+\beta u(\mathbf{r}^n;\lambda-\delta\lambda)}\right\rangle}\Bigg\rangle_{\mathbf{R}^N,\lambda}\end{aligned} \tag{6}$$

After expanding the exponentials in terms of $\delta\lambda$ and discarding all terms higher than linear in $\delta\lambda$ (see Appendix A for details), one obtains

DOI: 10.1021/acs.jctc.5b00180
J. Chem. Theory Comput. 2015, 11, 3547−3560

$$\frac{\mathrm{d}\nabla U(\mathbf{R}^N;\lambda)}{\mathrm{d}\lambda} = \left\langle M^{\dagger}\left(\frac{\mathrm{d}\nabla u(\mathbf{r}^n;\lambda)}{\mathrm{d}\lambda}\right) - \frac{\beta}{N_{\mathrm{CG}}}\left(\frac{\mathrm{d}u(\mathbf{r}^n;\lambda)}{\mathrm{d}\lambda} - \left\langle \frac{\mathrm{d}u(\mathbf{r}^n;\lambda)}{\mathrm{d}\lambda}\right\rangle_{\mathbf{R}^N,\lambda}\right) M^{\dagger}(\nabla u(\mathbf{r}^n;\lambda))\right\rangle_{\mathbf{R}^N,\lambda} \tag{7}$$

where N_{CG} is the number of CG sites in order to make the sensitivity intensive. This equation is a self-consistent iterative (SCI) single point formula because although the left-hand side seems optimistically like it could be computed in a variational approximation by performing FM on the right-hand side, this is actually not correct. The term $\langle \mathrm{d}u(\mathbf{r}^n;\lambda)/\mathrm{d}\lambda\rangle_{\mathbf{R}^N,\lambda}$ is exactly the many-body function that the formula is meant to calculate, and therefore, the equation must be solved iteratively: after each variational calculation step to find the left-hand side, $\langle \mathrm{d}u(\mathbf{r}^n;\lambda)/\mathrm{d}\lambda\rangle_{\mathbf{R}^N,\lambda}$ must be reevaluated framewise using the integrated form of the new left-hand side to generate new target derivatives, and a new variational calculation must be run. The process repeats until self-consistency. Note that FM calculates a potential up to an additive constant. Normally, this constant has no physical effect, but in this case, the constant is important in the nonlinear term containing $(\mathrm{d}u/\mathrm{d}\lambda - \langle \mathrm{d}u/\mathrm{d}\lambda\rangle)$. We therefore apply a configurationally independent constant correction to the difference $(\mathrm{d}u/\mathrm{d}\lambda - \langle \mathrm{d}u/\mathrm{d}\lambda\rangle)$ such that its average over all frames is zero. This amounts to a single step of direct scalar matching used to seed the iterative FM calculations; the scalar does not affect the distributions of configurations in sensitivity-corrected models.

Both the SCB and SCI single point formulas have the same first term on the right-hand side, which can be considered the naïve sensitivity because it neglects any nonpairwise effects on the CG potential and force field. Interestingly, this is what one would obtain if one reanalyzed a trajectory using a different parameter set as in the RFDs but neglected to apply the reweighting factor. This is in effect what was reported in ref 9. One can see that if the second set of terms on the right-hand side of both single point formulas were to be zero, this naïve sensitivity would in fact be the correct sensitivity. Thus, differences between the naïve sensitivity and the single point formulas reflect the importance of the correlation correction to the naïve sensitivity. Differences between the SCI and SCB equations reflect the importance of basis set effects in determining which correlations should be used to correct the naïve sensitivity for approximate models.

Even though these formulas both capture correlated many-body effects of the sensitivity, they do so in different ways. In the SCI single point formula, the correction to the naïve sensitivity is like a transport term because it is the product of the mapped forces and the deviations in $\mathrm{d}u/\mathrm{d}\lambda$; it measures the amount the FG distributions corresponding to each CG distribution are pushed around "underneath" the CG configuration. In the SCB single point formula, this correction is the product of the deviation in $\mathrm{d}u/\mathrm{d}\lambda$ and the deviation in the forces, making it a covariance term that closely echoes the covariance corrections to the naïve sensitivity found in the literature for single resolution sensitivity.[15] A practical difference between the two single point formulas is that the SCB averages $\langle \mathrm{d}u(\mathbf{r}^n;\lambda)/\mathrm{d}\lambda\rangle$ over the entire FG ensemble, requiring no iteration, whereas the SCI averages $\langle \mathrm{d}u(\mathbf{r}^n;\lambda)/\mathrm{d}\lambda\rangle$ conditionally on the CG ensemble that needs to be reevaluated based on the most recent estimate from the previous iteration. These differences in averaging are consistent with the differing applications of basis sets made in the derivation of each model. Both approaches become equivalent in the limit of a complete basis set, but for a finite basis set, the SCB formula describes a practically useful sensitivity; the SCI formula is better used as a diagnostic for understanding the physics of renormalized many-body effects.

B. Simulation and Fitting Details and Conditions. Molecular dynamics (MD) simulations were performed on AA methanol and 1 M sodium chloride systems in LAMMPS.[46−48] All systems were run with a 1 fs time step and used nonbonded Lennard-Jones (LJ) interactions with a radial cutoff of 1.0 nm as well as particle-particle particle-mesh (PPPM) electrostatic interactions. Both systems were equilibrated by simulating them for 5 ns at constant NPT at 1 atm and 300 K, setting their volume to the average of the last 2 ns of NPT simulation, and then simulating them for at least 1 ns at constant NVT at 300 K. Subsequent sampling for modified parameters was started from this equilibrated configuration but allowed to evolve for an additional 1 ns before sampling. The OPLS[49] methanol system of 1,000 molecules was sampled for 2 ns with configurations recorded every 250 fs, consistent with other studies.[23] For the sodium chloride system, 20 sodium and 20 chloride ions were simulated using Joung and Cheatham's[50] parametrization solvated in 3330 SPC/E[51] water molecules for 20 ns with configurations recorded every 200 fs, consistent with other studies.[52] The methanol system was coarse-grained to one site per molecule using a center of mass mapping, as in previous work.[23] The sodium chloride system was coarse-grained by eliminating all water molecules to create a solvent-free model.[52] All CG forces, potentials, and sensitivities were calculated using the MS-CG FM code with a nonbonded cutoff of 1.0 nm and sixth order spline basis functions with a resolution of 0.07 nm. CG simulations were started from the mapped version of the final configuration for the sampling run. A total of 1,000 CG timesteps were allowed for equilibration and randomization. Configurations were sampled every 1,000 CG timesteps for both systems with sampling runs of 2×10^6 CG timesteps for CG methanol and 2×10^7 CG timesteps for CG solvent-free sodium chloride.

Independent samples and reweighted potentials were calculated for changes to all LJ epsilon, LJ sigma, and partial charge parameters. In units of kcal/mol for LJ epsilon, Angstroms for LJ sigma, and e, the fundamental charge, for charge, CG potentials were calculated with positive or negative changes in one parameter of 0.001, 0.002, 0.005, 0.010, and 0.020. Changes to the charge of one atom type were offset by changes to the charge on an adjacent atom type to keep each molecule charge neutral. For methanol, this meant moving charges on the carbon and the neighboring methyl hydrogens or the oxygen and the neighboring hydroxyl hydrogen for methanol. For sodium chloride, this meant moving charges on the ions or within the water molecule. For the graphs comparing the single point formulas to the MTFDs and RFDs, the confidence ranges for MTFD and RFD curves were determined by integrating the 95% confidence interval calculated for all pairs of FDs within 0.005 parameter units. Confidence ranges for the single point formulas and the RFDs in these curves were likewise calculated by integrating the 95% confidence interval from 5 replica simulations. The confidence range for all of the independent trajectories corresponds to the

DOI: 10.1021/acs.jctc.5b00180
J. Chem. Theory Comput. 2015, 11, 3547−3560

integrated 95% confidence interval of 6 replicas using the original parametrization.

Comparing the effectiveness of these sensitivity formulas for transferring potentials required comparing predicted potentials (i.e., original potentials plus the sensitivity with respect to a parameter times the change in the parameter) to the CG potentials obtained from both (1) independent trajectories using an actually modified parameter set and (2) Boltzmann reweighting the original trajectory to the modified parameter set. The difference in these modified CG potentials via sensitivity, via reweighting, and via independent trajectories from the CG potential with the original parameters is quantified by integrating the absolute difference multiplied by the RDF and divided by the range of integration. This gives a single number summary (in energy units) of how different the variously transferred potentials are from the original potential for a given change in parameters. In this section, the confidence ranges for each point were calculated by propagating the uncertainty from the potentials through each of the operations in eq 9. The uncertainty of each point of the potentials was calculated as the root-mean-square (RMS) fluctuations of six independent trajectories. This uncertainty in the potential was used to calculate the uncertainty in the difference of the potentials at each point, combining the uncertainties via an RMS calculation (also referred to as error propagation in quadrature). Then, this uncertainty in the difference was scaled by the magnitude of the RDF at that point and the normalization before combining via an RMS calculation to give the uncertainty used to calculate the confidence ranges shown for each point.

III. RESULTS AND DISCUSSION

A. Numerical Finite Differences. Before the performance of the single point formulas developed in this work is evaluated, it is worth evaluating the noise and performance of the existing numerical FD calculations. Figure 1 compares the MTFD and the RFD with confidence ranges for the sensitivity of the single site methanol CG potential to changes in the charge on the hydroxyl's hydrogen. As expected, both estimates agree within the confidence ranges for sufficiently small changes to the charge, but the RFD has significantly smaller confidence ranges than the MTFD, which is expected because small differences in the MTFD denominator magnify sampling noise. In fact, the RFD confidence ranges are more than 100× smaller than for MTFD. For the purposes of initially verifying the precision of our single point formula, only RFDs with confidence ranges will be shown because it is expected that any predicted sensitivity that agrees with the RFD within the confidence ranges will also agree with the MTFD. However, this is not always the case, especially when the RFD calculations are strongly biased. Thus, to demonstrate the accuracy of the single point formulas, comparisons will be made to MTFDs or independent trajectories (IT) later in the paper.

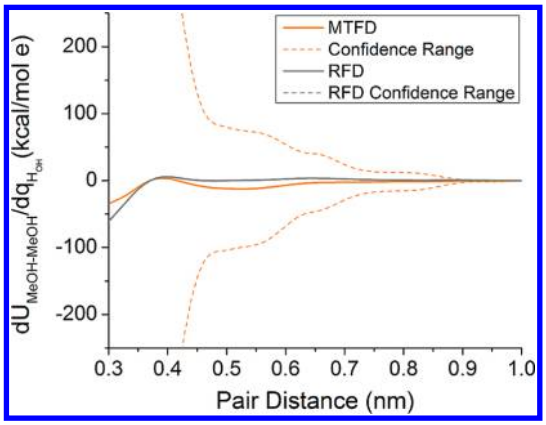

Figure 1. Comparison of multitrajectory FD (MTFD) and reweighted FD (RFD) for the sensitivity of the MeOH CG potential to changes in the charge on the hydroxyl hydrogen (H_{OH}). Confidence ranges show the relative noise of each estimated sensitivity, as defined in the main text. The RFD confidence range is so small relative to the MTFD confidence range that it is not distinguishable from the RFD curve on this scale.

B. Single Site Methanol. *Sensitivity Comparisons.* The sensitivities calculated using the SCB single point formula are compared to the SCI single point formula as well as the RFD sensitivity estimates with confidence ranges in Figure 2. For LJ epsilon (Figure 2a and b) and sigma (Figure 2c), the SCB and SCI estimates superimpose, indicating that nonpair-representable many-body effects play little role in the pair-representable part of these sensitivities. The SCB and SCI estimates for these graphs are generally within the shown confidence range and only slightly overestimate the magnitude of the sensitivity at short interaction pair distances. For sensitivity to charge (Figure 2d), the SCI estimate is significantly different from either the SCB estimate or the actual RFD sensitivity. This difference between SCB and SCI estimates indicates that significant multibody correlations are important for charge interactions and correlations. These observations agree with and clarify prior work that indicated that CG potentials are significantly less transferable, in the naïve sense, for charge interactions than epsilon and sigma interactions because of the significant multibody correlations present.[53]

Predicted Potentials. As mentioned in Section II, potentials can be predicted using sensitivities from either of the single point formulas using

$$U(\mathbf{R}^N;\ \lambda + \delta\lambda) = U(\mathbf{R}^N;\ \lambda) + \delta\lambda\left(\frac{\mathrm{d}U(\mathbf{R}^N;\ \lambda)}{\mathrm{d}\lambda}\right) \tag{8}$$

which is a simple correction to the original potential that is linear in $\mathrm{d}\lambda$. The magnitude of change in CG interaction potential from the reference (REF) parametrization as plotted in Figure 3 was calculated as

$$|\Delta U| = \frac{1}{R_H - R_L}\int_{R_L}^{R_H} \mathrm{d}R\,|U_{\mathrm{PRED}}(R;\ \lambda + \delta\lambda) - U_{\mathrm{REF}}(R;\ \lambda)|g_{\mathrm{REF}}(R) \tag{9}$$

where $g_{\mathrm{REF}}(R)$ is the radial distribution function of the reference parametrization, $U_{\mathrm{PRED}}(R;\lambda + \delta\lambda)$ is the interaction potential at a nonreference parametrization either from FMing independent FG NVT trajectories with the modified parametrization or using eq 8 with the sensitivity calculated using RFD, SCI, or SCB formulas. Figure 3 shows the difference in potentials for different $\delta\lambda$'s from the original ($\delta\lambda = 0$) potential as described in Section II. For the epsilon graph (Figure 3a), both the SCB and SCI curves agree with the reweighted curve for small differences—in the linear regime. It is remarkable that both sensitivities have the same average slope as the curve for the CG potential determined for the new parameters with independent trajectories for changes of only 0.01 kcal/mol. For the sigma graph (Figure 3b), the reweighted curves are

DOI: 10.1021/acs.jctc.5b00180
J. Chem. Theory Comput. 2015, 11, 3547−3560

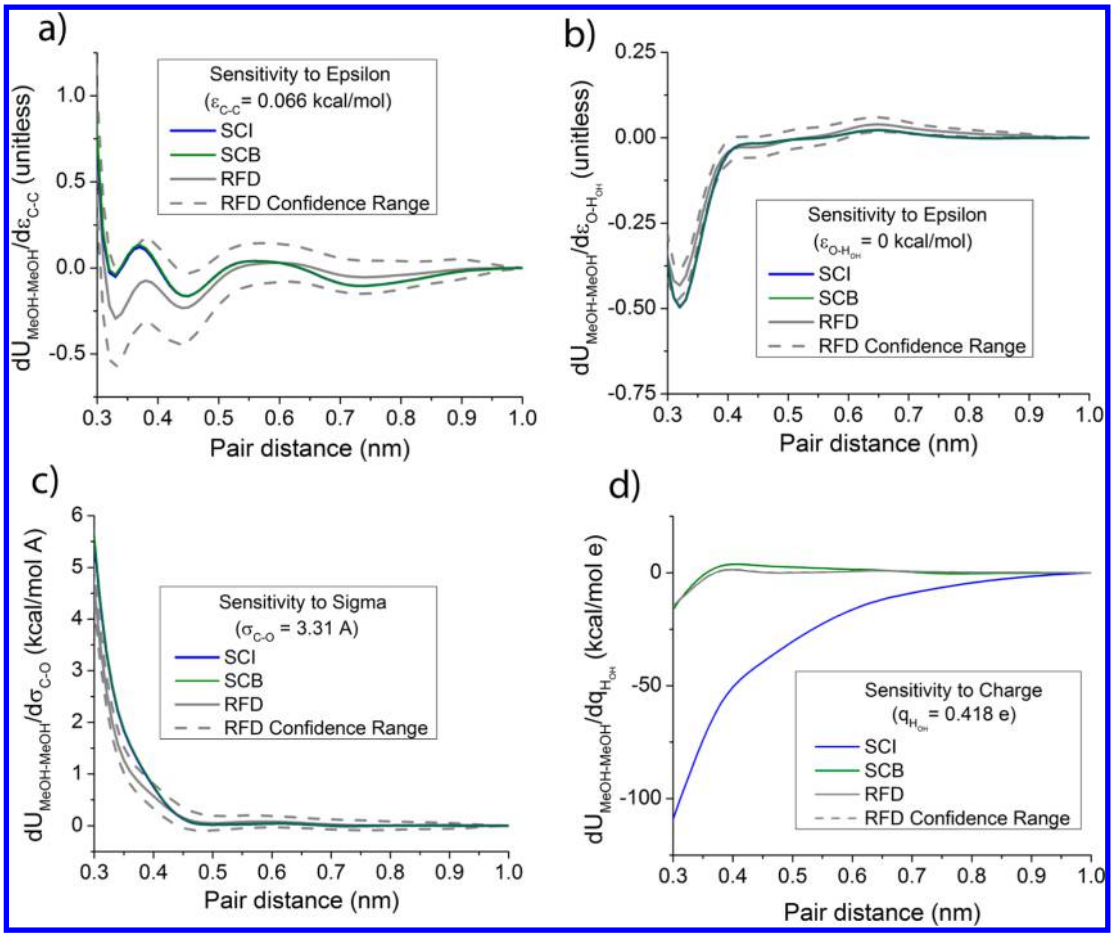

Figure 2. Comparison of methanol sensitivity estimates for different interaction parameters between RFD, self-consistent iterative (SCI) single point, and self-consistent basis (SCB) single point calculations. Sensitivities are taken with respect to (a) carbon−carbon (C−C) LJ epsilon, b) oxygen−hydroxyl-hydrogen ($O-H_{OH}$) LJ epsilon, (c) carbon−oxygen (C−O) LJ sigma, and (d) hydroxyl hydrogen (H_{OH}) charge interaction parameters. RFD confidence ranges are calculated as defined in the main text. The RFD confidence range for (d) is so small that it is not visible on this scale.

nonlinear, but the SCB sensitivity appears to have the same average slope as the SCI sensitivity and the reweighted curve. The independent trajectories curve has a similar initial slope to the single point sensitivities but is below the single point sensitivities for larger changes. This is somewhat expected because as perturbations increase, systems will typically make compensating changes that result in a concave response. For the charge graph (Figure 3c), the reweighted curve shows nonlinearity, but the SCB curve is nonetheless reasonably consistent with the reweighted curve. As expected from the sensitivity comparisons, the SCI curve drastically overestimates the change in potential. Although neither of the single point sensitivities matches the independent trajectories for charge, neither does the reweighted curve beyond 0.005 e, indicating significant sampling changes in response to charge modification that may be the result of changes in complex many-body and long-range effective interactions.

CG Simulations. Another way to assess the accuracy of these predicted potentials is to compare the RDFs generated from CG simulations using both the actual CG potential and the potentials predicted from both sensitivity formulas. Figure 4 shows the RDF for a selected set of $\delta\lambda$. It is clear that any slight errors shown in Figure 3 for predictions across epsilon (Figure 3a) and sigma (Figure 3b) values do not lead to noticeable errors in the RDFs. For predictions across charge (Figure 3c) values, the RDF from the SCB predicted potential has only minor deviations in the height of the first peak and valley from the actual RDF. The agreement of the RDF from the SCB predicted potential bodes well for the application of sensitivity for generating predicted potentials. However, there is a limit to how far one can use these predicted potentials, which corresponds to the breakdown of the first order approximation of the sensitivity outside the linear regime. Figure 3d−f shows that, for sufficiently large changes in the FG interaction parameters, the magnitude of the RDF peaks and valleys differ significantly from those of the RDF obtained using the actual CG potential with the modified interaction parameters. Nonetheless, the RDFs for larger interaction parameter changes continue to show good agreement with the location of the peaks and valleys for the first two solvation shells.

C. Solvent-Free Sodium Chloride. *Sensitivity Comparisons.* The sensitivities calculated using the SCB single point formula are compared to the SCI single point formula and the RFD sensitivity estimates with confidence ranges in Figure 5. For epsilon (Figure 5a and b) and sigma (Figure 5c), the SCB and SCI sensitivities are entirely within the shown confidence ranges. It is interesting to note that the magnitude of the SCI sensitivity is less than the magnitude of the SCB sensitivity when they deviate in Figure 5a−c at short interaction distances, indicating that the SCB covariance correction is greater than

DOI: 10.1021/acs.jctc.5b00180
J. Chem. Theory Comput. 2015, 11, 3547−3560

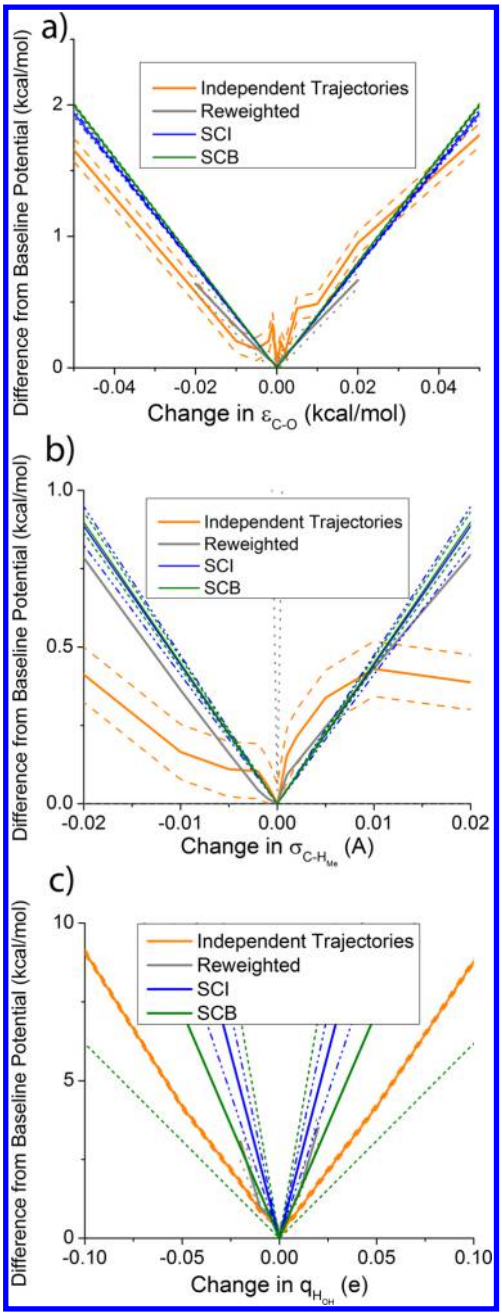

Figure 3. Magnitude of change in methanol CG interaction potential from OPLS parametrization, calculated (see eq 9) as a weighted average absolute difference in predicted potential from a reference potential weighted by the reference RDF, for predictions via independent trajectories, reweighting, and the two single point sensitivities SCI and SCB. Predictions are compared for changes in (a) carbon−oxygen (C−O) LJ epsilon, (b) carbon−methyl-hydrogen ($C-H_{Me}$) LJ sigma, and (c) hydroxyl hydrogen (H_{OH}) charge interactions.

the SCI transport correction because of differences in the amount of sensitivity captured due to the different basis set considerations between the two formulas. For sensitivity to charge (Figure 5d), the SCI estimate is significantly below the actual RFD sensitivity and the SCB sensitivity, which is above the RFD confidence range for large interaction distances and below it for intermediate interaction distances. However, both the SCB and SCI sensitivities show much better qualitative agreement for the sensitivity to charge in the sodium chloride system than in the methanol system, suggesting that the effects of electrostatics are more pair-representable in this system.

Predicted Potentials. Figure 6 shows the difference in potentials from eq 9 for different $\delta\lambda$'s from the original ($\delta\lambda = 0$) potential as described in Section II. For the epsilon graph (Figure 6a), the SCB curve agrees with the reweighted curve for small changes until the nonlinearities appear in the reweighted curve, where bias is more of a problem. The SCB curve is also in the same range as the independent trajectories for large changes. The SCI curve deviates from both reference curves for sizable changes but appears to have the same initial slope as the independent trajectories, which is likely within the linear regime. For the sigma graph (Figure 6b), the SCB curve shows even better agreement with the reweighted curve and the average slope of the independent trajectories curve than in Figure 6a. The large difference between the SCI and SCB curves indicates the importance of CG basis set effects in capturing the correlations important for larger changes in parameters. For the charge graph (Figure 6c), the reweighted curve looks quite linear and shows agreement with the independent trajectories only for small changes. The difference between the SCB and reweighted curves from the independent trajectories may be due to underestimation of many-body charge screening effects that the reweighted and SCB methods do not incorporate due to configurational sampling bias. The SCB curve agrees with the reweighted curve but both overestimate changes in the potential. The SCI curve here seems to have the same average slope as the independent trajectories for positive and negative changes, indicating either less bias or a cancellation of errors.

CG Simulations. Figure 7 shows the RDFs for a selected set of $\delta\lambda$. For the sensitivity to epsilon example, the heights of the first peaks predicted from the single point sensitivities for the Na−Na and Cl−Cl RDFs (not shown, see SI) are slightly overstructured, but the opposite is true for the Na−Cl RDF (Figure 7a). The opposing errors in the RDFs and potentials illustrate the additional problems of fitting the three nonbonded interactions simultaneously. For the sensitivity to sigma example (Figure 7b), the RDF from the SCB predicted potential seems to be in agreement with the actual CG RDF with only minor understructuring of the contact-ion pair. When it comes to the sensitivity to charge (Figure 7c), it is clear that the errors in the sensitivity of the potential carried through to the RDFs as they are all uniformly overstructured. It is not all that surprising that the charge sensitivities from the single point formulas overstructure the ions because this amounts to an underestimate of a many-body screening effect from waters that were coarse-grained out of the simulation. This continues to get worse for larger changes to the charges on the water (Figure 7f). The corrections to the water screening and structure are likely manifested in many-body interactions that are beyond the range of these first order, pair-representable sensitivities. Fortunately, the agreement between the RDFs to epsilon (Figure 7d) and sigma (Figure 7e) parameters is quite good over a larger range of parameter changes. As with the methanol system, the heights of the RDF peaks and valley differ only slightly for epsilon and sigma given the magnitude of the parameter change, whereas the location of the peaks and valley agree quite well. Thus, using the sensitivities from less highly correlated interactions, such as the LJ nonbonded interactions, appears to lead to reasonably predicted CG potentials and CG RDFs.

DOI: 10.1021/acs.jctc.5b00180
J. Chem. Theory Comput. 2015, 11, 3547−3560

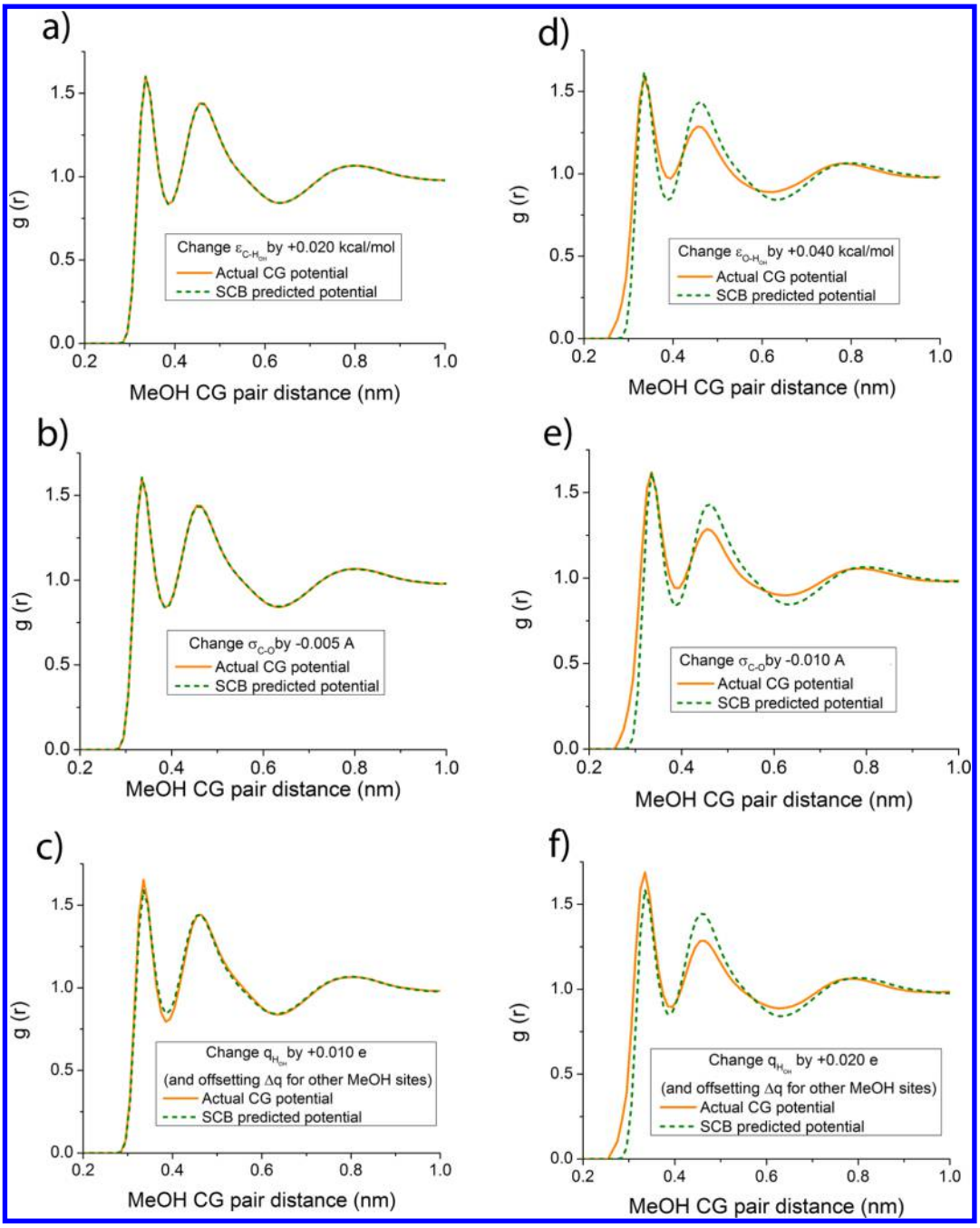

Figure 4. Radial distribution functions (RDFs) from CG methanol simulations. (a) Changing carbon−hydroxyl-hydrogen ($C-H_{OH}$) LJ epsilon interaction parameter by 0.020 kcal/mol. (b) Changing carbon−oxygen (C−O) LJ sigma interaction parameter by −0.005 Å. (c) Changing the hydroxyl hydrogen's charge by +0.010 e and applying neutralizing charges on the other methanol FG sites. (d) Changing carbon−hydroxyl-hydrogen ($C-H_{OH}$) LJ epsilon interaction parameter by 0.040 kcal/mol. (e) Changing carbon−oxygen (C−O) LJ sigma interaction parameter by −0.010 Å. (f) Changing the hydroxyl hydrogen's charge by +0.020 e and applying neutralizing charges on the other methanol FG sites.

D. Discussion. In general, the sensitivities calculated with respect to LJ epsilon parameters show excellent agreement with the RFD sensitivities and the CG RDFs for both the CG methanol and solvent-free sodium chloride systems. The agreement in the difference from the baseline potential in Figure 3a, even well outside the linear regime, is particularly noteworthy. The slightly more correlated sensitivities with respect to sigma parameters showed good agreement for the CG methanol system, and better agreement than in the sodium chloride system that is more highly coarse-grained. However, the charge sensitivities are only qualitatively correct, reflecting the highly complex many-body correlations due to these long-range interactions. In the sodium chloride system, this was reflected in the overstructuring of the CG ion pair RDFs, but the fact that sensitivities to the charge on the atoms in the implicit water molecules are reasonable is promising. Unfortunately, agreement with RFDs implies that although these formulas significantly improve the signal-to-noise ratio of reweighted finite differences, in many cases they do not address the problem of bias. This work reveals that bias in these estimators, not noise, is the next truly difficult problem to overcome, and it will not be overcome simply with more data as

DOI: 10.1021/acs.jctc.5b00180
J. Chem. Theory Comput. 2015, 11, 3547−3560

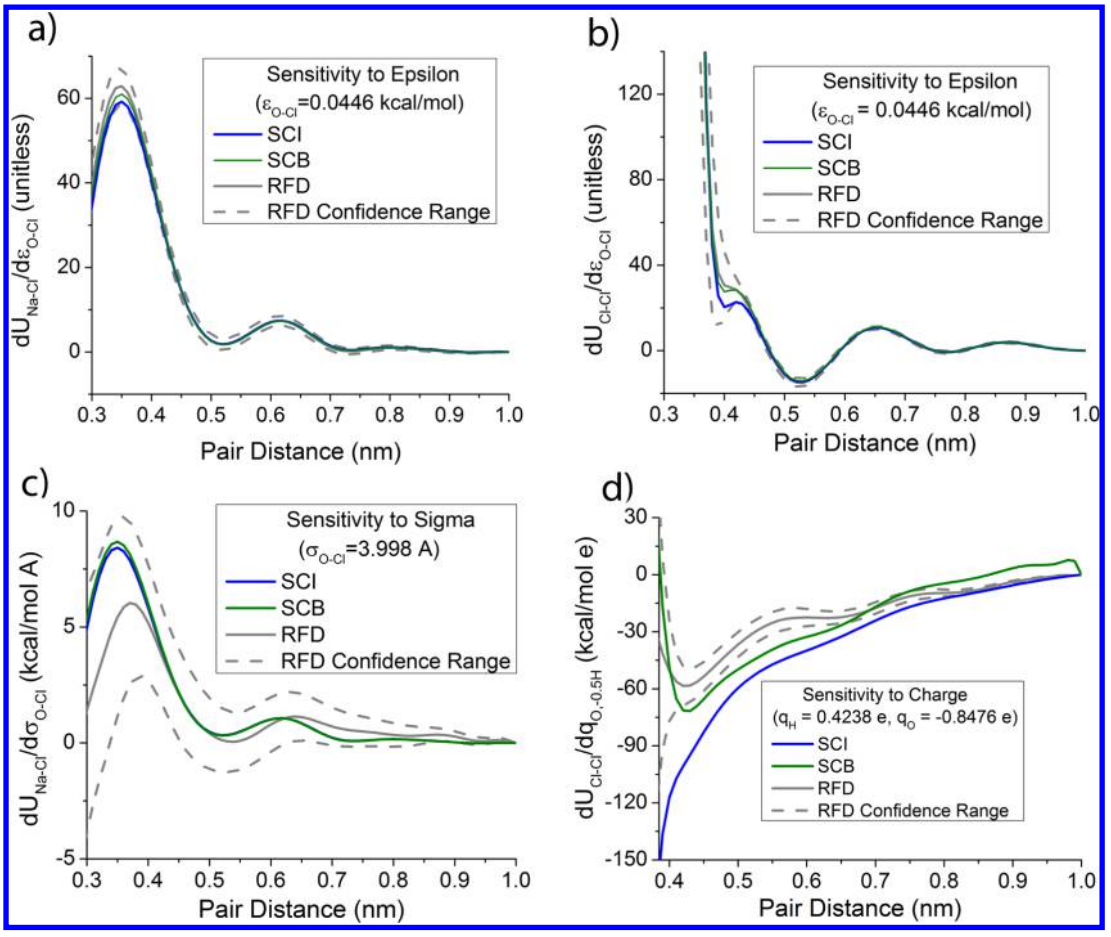

Figure 5. Comparison of solvent-free sodium chloride Na−Na, Na−Cl, and Cl−Cl interaction potential sensitivities estimated for different interaction parameters between RFD, SCI single point, and SCB single point calculations. Sensitivities of the (a) Na−Cl CG potential to the FG oxygen−chloride (O−Cl) LJ epsilon, (b) Cl−Cl CG potential to the FG oxygen−chloride (O−Cl) LJ epsilon, (c) Na−Cl CG potential to the oxygen−chloride (O−Cl) LJ sigma, and (d) Cl−Cl CG potential to the water oxygen and hydrogen charge interactions.

we attempted with this per-particle derivative-matching approach; bias is better dealt with by acquiring better data[54] or more sophisticated estimators.[55−57]

One can expect that the SCB sensitivities will be the most accurate and predictive when the relevant interaction is short-range and does not involve many-body correlations, as is the case for any short-range pair interaction modeling van der Waals interactions, such as the Lennard-Jones potential. In contrast, interactions that are long-range and involve many-body correlations, such as charge interactions, are expected to be less accurate and less predictive. Although the sensitivity of intramolecular interactions, such as bonds, angles, and dihedrals, were not investigated, physical considerations suggest that these sensitivities will not be as well-behaved as those for Lennard-Jones parameters because intra-CG-site interactions affect the CG interactions only indirectly through multiatom correlations, but on the other hand, they should be better than the sensitivities for charge interactions because intramolecular interactions are short ranged. Likewise, sensitivity of state parameters, such as temperature and volume as well as their conjugate observables entropy and pressure, were not investigated here, but we expect the sensitivities to these parameters to be inaccurate because the relevant interactions are long-range and involve many-body correlations that may not be pair-representable.

One way to verify these heuristics is to compare the SCB estimate to the SCI estimate for each parameter of interest in a given system. If the SCB and SCI estimates agree, as in Figure 2a−c and Figure 5 a−c, then the many-body correlations that lead to the correction of the naïve sensitivity, which the two formulas estimate differently, are well-represented in the chosen basis set. This means that the SCB sensitivity is more likely to be accurate and predictive. This feature implies that these SCI and SCB formulas can be used diagnostically to evaluate hypotheses about transferability even when they do not provide accurate linear sensitivity measurements. However, when they do, they also provide previously infeasible checks on the precise size of the linear regime: in that case, this regime will be precisely the range over which the RFD and SCB estimates agree.

The times when the SCB and SCI single point formulas differ in their sensitivity estimates are significant because the two capture correlated many-body effects in different ways. In particular, any significant correction to the naïve sensitivity from either single point formula indicates the presence of significant multibody effects and correlations in the sensitivity to that parameter. Differences between them, moreover, specifically indicate that the nonrepresentable many-body effects are folded into the corresponding representable force field for a given basis, which are sensitive to the parameter under study in ways that cannot be represented within that

DOI: 10.1021/acs.jctc.5b00180
J. Chem. Theory Comput. 2015, 11, 3547−3560

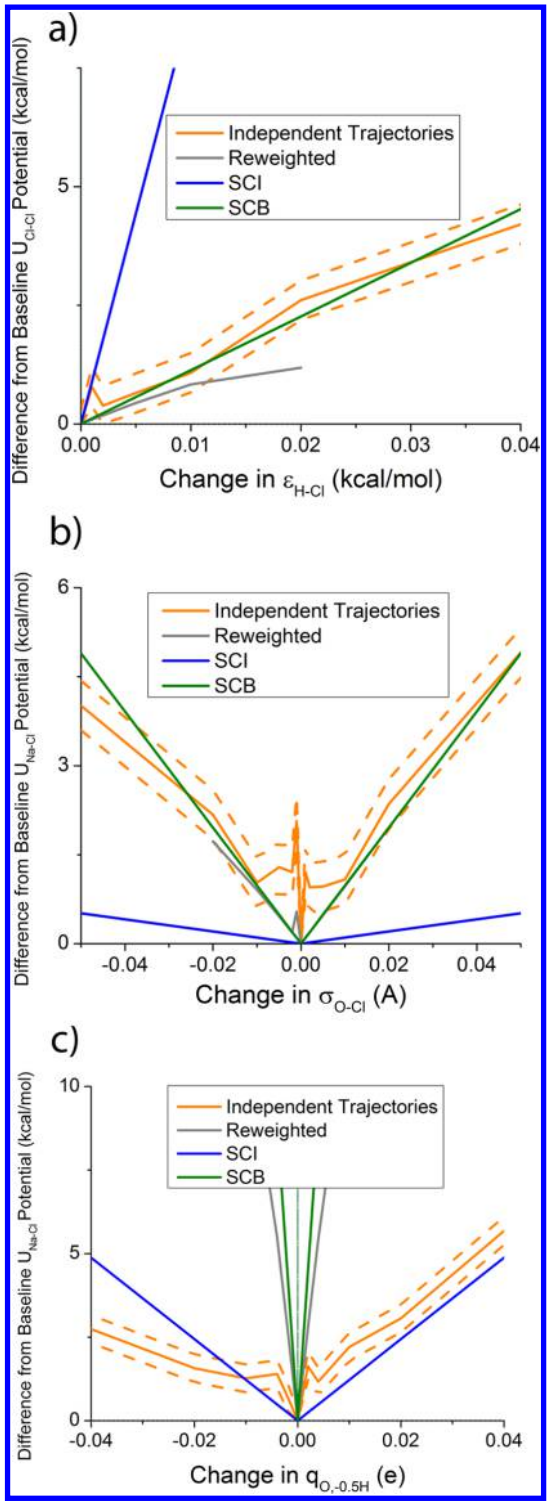

Figure 6. Magnitude of change in sodium chloride CG interaction potential from SPC/E water and Joung and Cheatham NaCl parametrization, calculated as a weighted average absolute difference in predicted potential from a reference potential weighted by the reference RDF for predictions via independent trajectories, reweighting, and the two single point sensitivities SCI and SCB. Predictions of (a) U_{Cl-Cl} to changes in hydrogen−chloride (H−Cl) LJ epsilon, (b) U_{Na-Cl} to changes in oxygen−chloride (O−Cl) LJ sigma, and (c) U_{Na-Cl} to changes in water hydrogen and oxygen charges are compared.

basis set. The difference in the estimates for the sensitivity to epsilon in the solvent-free NaCl system, but not the CG methanol system, reflects that the NaCl system is more highly coarse-grained as expected. Also, the difference between the SCB and SCI sensitivity estimates for charge interactions quantifies and confirms the dependence of the effective pair potential on the significant and complex many-body correlations among long-range interactions that had been hypothesized previously in the literature.[53]

Noise and modeling error can still remain problematic even when these formulas perform without significant bias. Approaches previously used to improve the ability of force matching to deal with these problems could also potentially be brought to bear to improve these sensitivity calculations. For instance, regularization of these sensitivity estimators similar to Lu et al.'s approach could improve the performance of these estimates with noisy data.[45,58] Alternatively, it may be that structural differences between the CG and FG models due to the use of a finite basis set lead to prediction errors that could be ameliorated via recalculation of the input sensitivity derivatives, $M^{\dagger}(\mathrm{d}\nabla u(\mathbf{r}^n;\lambda)/\mathrm{d}\lambda)$ and $\mathrm{d}u(\mathbf{r}^n;\lambda)/\mathrm{d}\lambda$, using statistics from CG sampling as well as FG sampling as in iterative FM and iterative g-YBG approaches.[59−61]

More systematic studies of the differences between calculations by these two formulas may reveal more of the character of important many-body effects in various systems. Although we focused on well-known interaction parameters here, it is possible to use these formulas to investigate the addition of arbitrary biases to FG models to examine the effects of arbitrary correlations on the representable correlations in a system. This could reveal interesting experimental control parameters for fine-grained systems, (e.g., in discovering manipulable fields conjugate to CG tetrahedrality correlations in water).[62−64] Furthermore, although we studied only pair-representable force fields here and considered only fixed CG basis sets, we can also use it as a criterion for basis set quality, indicating that it could also be useful for basis set design. One can use these formulas with arbitrarily complex CG basis sets and the comparisons between SCI and SCB formulas in various basis sets to choose the ones that will result in the most transferable models across a given parameter space.

Finally, the results indicate that the calculation of sensitivities to nonbonded interaction parameters is good for generating predicted potentials, especially for sensitivities to LJ epsilon and sigma interaction parameters. A direct extension of this work would be to calculate thermodynamic derivatives by repeating the derivations in Section II with $\lambda = \beta$, the thermodynamic temperature. Because the formulas can only be used to calculate sensitivities to continuous parameters, sensitivities to volume $\lambda = V$ could be calculated in the constant NPT and μPT ensembles, whereas sensitivities to concentration could be calculated via sensitivities to chemical potential $\lambda = \mu$ in the constant μPT and μVT grand canonical ensembles. Another extension of the work would be to calculate the sensitivity of other CG properties or observables, such as the RDF g(r) by applying a chain rule, where the sensitivity of the CG property or observable to the CG potential would be multiplied by the sensitivity of the CG potential to FG interaction parameters as presented in this work.

IV. CONCLUSIONS

In this article, new reweighting-free formulas for the calculation of the sensitivity of CG potentials and force fields to changes in

DOI: 10.1021/acs.jctc.5b00180
J. Chem. Theory Comput. 2015, 11, 3547−3560

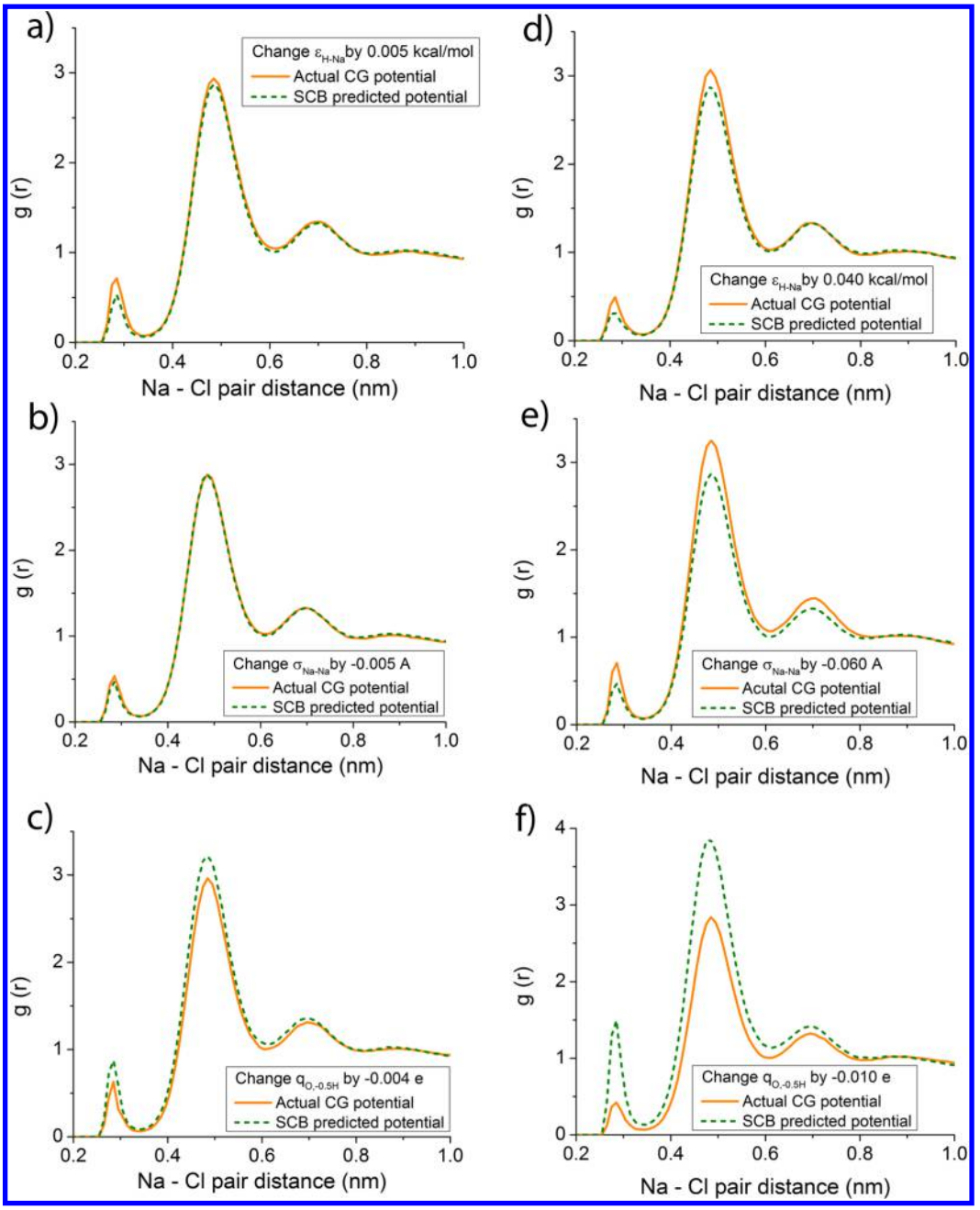

Figure 7. Radial distribution functions (RDFs) from CG sodium chloride simulations for the Na−Cl pair distance. (a) Changing hydrogen−sodium (H−Na) LJ epsilon interaction parameter by 0.005 kcal/mol. (b) Changing sodium−sodium (Na−Na) LJ sigma interaction parameter by −0.005 Å. (c) Changing the water oxygen charge by −0.004 e and the water hydrogen by +0.002 e. (d) Changing hydrogen−sodium (H−Na) LJ epsilon interaction parameter by 0.040 kcal/mol. (e) Changing sodium−sodium (Na−Na) LJ sigma interaction parameter by −0.060 Å. f) Changing the water oxygen charge by −0.010 e and the water hydrogen by +0.005 e.

the underlying FG model's interaction parameters and state point were presented that require only a single trajectory for calculation. In the results, the SCB estimates predicted sensitivities to LJ epsilon and sigma parameters that were quantitatively correct to within the confidence ranges from RFDs, representative of the practical state of the art. The single point formula does not require a priori knowledge of the linear sensitivity regime for a given parameter and can be useful in generating predicted CG potentials for other interaction parameters, as demonstrated by the agreement of the CG RDFs from independent trajectories with predicted potentials using this sensitivity. Of the predictive sensitivity measures examined here, the single point methods provide the lowest noise estimates of all, providing the same sensitivities as RFDs at reduced computational cost with comparable bias and without ambiguity concerning the size of the linear regime.

Finally, beyond their purely computational significance, these results also serve to shed light onto relatively unexplored subtleties of CG representability. Consideration of both the SCB and SCI formulas offers a new window into the fundamental theoretical problems of representing transfer of CG models between state points, providing a vivid example of how the change from FG model to FG model in the CG-representable part of the correlations may not always be the

DOI: 10.1021/acs.jctc.5b00180
J. Chem. Theory Comput. 2015, 11, 3547−3560

same as the CG-representable part of the change in correlations from FG model to FG model—even at the level of linear response. Although this is sometimes mentioned in discussions of the foundations of coarse-graining, that subtlety is rarely investigated as a practical effect with fundamental physical importance in its own right. However, establishing one's foundations is also an eminently practical thing to do. We hope this work will spur deeper investigations into the theoretical interplay between representability and transferability, two of the most important challenge areas in state of the art coarse-graining and CG modeling, in addition to providing new computational tools.

APPENDIX A: DERIVATION OF THE SCB SINGLE POINT FORMULA

The self-consistent basis single point sensitivity formula describes the derivative with respect to system parameters of variationally force matched finite-basis approximations to the true many-body free energy surface (FES). The usual force-matching normal equations for a potential of mean force (PMF) approximated as a linear combination of a set of basis functions ψ_d with coefficients ϕ_d and λ are

$$\frac{1}{N_t N}\sum_{t=1}^{N_t}\sum_{I=1}^{N}\frac{\mathrm{d}\psi_d}{\mathrm{d}\mathbf{R}_I}\times\sum_{d'}\frac{\mathrm{d}\psi_{d'}}{\mathrm{d}\mathbf{R}_I}\phi_{d',\lambda}=\frac{1}{N_t N}\sum_{t=1}^{N_t}\sum_{I=1}^{N}\frac{\mathrm{d}\psi_d}{\mathrm{d}\mathbf{R}_I}\times\mathbf{F}_I(\mathbf{r}_t^n;\lambda) \tag{A1}$$

where $\mathbf{F}_I$ are CGed forces from sampled atomistic configurations. This is an equation valid for sampling from a system with fixed parameter λ. To take the derivative of this with respect to λ, one must find a way to express the sampling density as a differentiable function of λ in this expression. One option is to assume all sampling is run at a reference λ_0 and then perform a weighted least-squares optimization using the reweighting factors (see eq 5 in the main text) rather than a uniformly weighted least-squares optimization. Using the usual equations for weighted least-squares, one obtains the normal equations

$$\begin{aligned}&\frac{1}{N_t N}\sum_{t=1}^{N_t}w(\mathbf{r}_t^n;\lambda,\lambda_0)\sum_{I=1}^{N}\frac{\mathrm{d}\psi_d}{\mathrm{d}\mathbf{R}_I}\times\sum_{d'}\frac{\mathrm{d}\psi_{d'}}{\mathrm{d}\mathbf{R}_I}\phi_{d',\lambda}\\&=\frac{1}{N_t N}\sum_{t=1}^{N_t}w(\mathbf{r}_t^n;\lambda,\lambda_0)\sum_{I=1}^{N}\frac{\mathrm{d}\psi_d}{\mathrm{d}\mathbf{R}_I}\times\mathbf{F}_I(\mathbf{r}_t^n;\lambda)\end{aligned} \tag{A2}$$

which are in principle valid for any λ with samples taken with respect to any λ_0, though of course only practical when λ is close to λ_0. First define

$$G_{d,d'}(\lambda,\lambda_0)=\frac{1}{N_t N}\sum_{t=1}^{N_t}w(\mathbf{r}_t^n;\lambda,\lambda_0)\sum_{I=1}^{N}\frac{\mathrm{d}\psi_d}{\mathrm{d}\mathbf{R}_I}\frac{\mathrm{d}\psi_{d'}}{\mathrm{d}\mathbf{R}_I} \tag{A3a}$$

$$b_d(\lambda,\lambda_0)=\frac{1}{N_t N}\sum_{t=1}^{N_t}w(\mathbf{r}_t^n;\lambda,\lambda_0)\sum_{I=1}^{N}\frac{\mathrm{d}\psi_d}{\mathrm{d}\mathbf{R}_I}\times\mathbf{F}_I(\mathbf{r}_t^n;\lambda) \tag{A3b}$$

Now, taking the derivative of both sides, one gets

$$\sum_{d'}G_{d,d'}(\lambda,\lambda_0)\frac{\mathrm{d}\phi_{d',\lambda}}{\mathrm{d}\lambda}=\frac{\mathrm{d}}{\mathrm{d}\lambda}(b_d(\lambda,\lambda_0)-\sum_{d'}G_{d,d'}(\lambda,\lambda_0)\phi_{d',\lambda*}) \tag{A4}$$

where $\lambda*$ is equal to λ, but does not change with λ in that expression. This is a force-matching-like equation for the change in the expansion coefficients, which gives the change in the PMF when multiplied by the basis functions. The equation matches the change from the true target forces, b_d, from the predicted forces with fixed PMF, $G_{d,d'}$ $\phi_{d'}$, and adjusted sampling.

Evaluating the derivatives is easiest after re-expanding the new notation

$$\begin{aligned}&\frac{1}{N_t N}\sum_{t=1}^{N_t}w(\mathbf{r}_t^n;\lambda,\lambda_0)\sum_{I=1}^{N}\frac{\mathrm{d}\psi_d}{\mathrm{d}\mathbf{R}_I}\times\sum_{d'}\frac{\mathrm{d}\psi_{d'}}{\mathrm{d}\mathbf{R}_I}\frac{\mathrm{d}\phi_{d',\lambda}}{\mathrm{d}\lambda}\\&=\frac{\mathrm{d}}{\mathrm{d}\lambda}\left(\frac{1}{N_t N}\sum_{t=1}^{N_t}w(\mathbf{r}_t^n;\lambda,\lambda_0)\sum_{I=1}^{N}\frac{\mathrm{d}\psi_d}{\mathrm{d}\mathbf{R}_I}\left(\mathbf{F}_I(\mathbf{r}_t^n;\lambda)-\sum_{d'}\frac{\mathrm{d}\psi_{d'}}{\mathrm{d}\mathbf{R}_I}\phi_{d',\lambda*}\right)\right)\\&=\frac{1}{N_t N}\sum_{t=1}^{N_t}\frac{\mathrm{d}w(\mathbf{r}_t^n;\lambda,\lambda_0)}{\mathrm{d}\lambda}\sum_{I=1}^{N}\frac{\mathrm{d}\psi_d}{\mathrm{d}\mathbf{R}_I}\left(\mathbf{F}_I(\mathbf{r}_t^n;\lambda)-\sum_{d'}\frac{\mathrm{d}\psi_{d'}}{\mathrm{d}\mathbf{R}_I}\phi_{d',\lambda*}\right)\\&\quad+\frac{1}{N_t N}\sum_{t=1}^{N_t}w(\mathbf{r}_t^n;\lambda,\lambda_0)\sum_{I=1}^{N}\frac{\mathrm{d}\psi_d}{\mathrm{d}\mathbf{R}_I}\frac{\mathrm{d}\mathbf{F}_I(\mathbf{r}_t^n;\lambda)}{\mathrm{d}\lambda}\\&=\frac{1}{N_t N}\sum_{I=1}^{N_t}w(\mathbf{r}_t^n;\lambda,\lambda_0)\beta\left(-\frac{\mathrm{d}u(\mathbf{r}_t^n;\lambda)}{\mathrm{d}\lambda}+\sum_{t'=1}^{N_t}w(\mathbf{r}_{t'}^n;\lambda,\lambda_0)\frac{\mathrm{d}u(\mathbf{r}_{t'}^n;\lambda)}{\mathrm{d}\lambda}\right)\\&\quad\times\sum_{I=1}^{N}\frac{\mathrm{d}\psi_d}{\mathrm{d}\mathbf{R}_I}\left(\mathbf{F}_I(\mathbf{r}_t^n;\lambda)-\sum_{d'}\frac{\mathrm{d}\psi_{d'}}{\mathrm{d}\mathbf{R}_I}\phi_{d',\lambda*}\right)\\&\quad+\frac{1}{N_t N}\sum_{t=1}^{N_t}w(\mathbf{r}_t^n;\lambda,\lambda_0)\sum_{I=1}^{N}\frac{\mathrm{d}\psi_d}{\mathrm{d}\mathbf{R}_I}\frac{\mathrm{d}\mathbf{F}_I(\mathbf{r}_t^n;\lambda)}{\mathrm{d}\lambda}\\&=\frac{1}{N_t N}\sum_{t=1}^{N_t}w(\mathbf{r}_t^n;\lambda,\lambda_0)\sum_{I=1}^{N}\frac{\mathrm{d}\psi_d}{\mathrm{d}\mathbf{R}_I}\left(\frac{\mathrm{d}\mathbf{F}_I(\mathbf{r}_t^n;\lambda)}{\mathrm{d}\lambda}\right.\\&\quad-\beta\left(\frac{\mathrm{d}u(\mathbf{r}_t^n;\lambda)}{\mathrm{d}\lambda}-\sum_{t'=1}^{N}w(\mathbf{r}_{t'}^n;\lambda,\lambda_0)\frac{\mathrm{d}u(\mathbf{r}_{t'}^n;\lambda)}{\mathrm{d}\lambda}\right)\\&\quad\left.\times\left(\mathbf{F}_I(\mathbf{r}_t^n;\lambda)-\sum_{d'}\frac{\mathrm{d}\psi_{d'}}{\mathrm{d}\mathbf{R}_I}\phi_{d',\lambda*}\right)\right)\end{aligned} \tag{A5}$$

which is just a weighted force matching for the newly apparent framewise sensitivities of forces in the parentheses, which are straightforward to calculate after force-matching first to find $\phi_{d,\lambda}$. Using a finite sum with some large number of samples provides a practical calculation scheme. Replacing the sums with ergodic averages, however, in the complete basis set limit, these normal equations correspond to eq 5, the covariance-like SCB formula described in the main text. In a finite basis set and in the long time limit, it corresponds to the λ-derivative of the g-YBG equations.

APPENDIX B: DERIVATION OF THE SCI SINGLE POINT FORMULA

The self-consistent iterative single point sensitivity formula is based on using a finite basis set to represent the per-particle-position derivatives of the full many-body sensitivity. To derive this, start with the definition of the many-body CG sensitivity

$$\frac{\mathrm{d}U(\mathbf{R}^N;\lambda)}{\mathrm{d}\lambda}=\left\langle\frac{\mathrm{d}u(\mathbf{r}^n;\lambda)}{\mathrm{d}\lambda}\right\rangle_{\mathbf{R}^N,\lambda} \tag{B1}$$

take the derivative with respect to all CG particle positions

$$\frac{\mathrm{d}\nabla_R U(\mathbf{R}^N;\lambda)}{\mathrm{d}\lambda}=\nabla_R\left(\frac{\int\mathrm{d}\mathbf{r}^n\delta(\mathbf{R}^N-M_{r\to R}(\mathbf{r}^n))\frac{\mathrm{d}u(\mathbf{r}^n;\lambda)}{\mathrm{d}\lambda}e^{-\beta u(\mathbf{r}^n;\lambda)}}{\int\mathrm{d}\mathbf{r}^n\delta(\mathbf{R}^N-M_{r\to R}(\mathbf{r}^n))e^{-\beta u(\mathbf{r}^n;\lambda)}}\right) \tag{B2}$$

apply the product rule to see

DOI: 10.1021/acs.jctc.5b00180
J. Chem. Theory Comput. 2015, 11, 3547−3560

$$\frac{\mathrm{d}\nabla_R U(\mathbf{R}^N;\lambda)}{\mathrm{d}\lambda} = \left(\frac{\int \mathrm{d}\mathbf{r}^n \nabla_R \delta(\mathbf{R}^N - M_{r\to R}(\mathbf{r}^n)) \frac{\mathrm{d}u(\mathbf{r}^n;\lambda)}{\mathrm{d}\lambda} e^{-\beta u(\mathbf{r}^n;\lambda)}}{\int \mathrm{d}\mathbf{r}^n \delta(\mathbf{R}^N - M_{r\to R}(\mathbf{r}^n)) e^{-\beta u(\mathbf{r}^n;\lambda)}} \right) - \left\langle \frac{\mathrm{d}u(\mathbf{r}^n;\lambda)}{\mathrm{d}\lambda} \right\rangle_{\mathbf{R}^N,\lambda} \left(\frac{\int \mathrm{d}\mathbf{r}^n \nabla_R \delta(\mathbf{R}^N - M_{r\to R}(\mathbf{r}^n)) e^{-\beta u(\mathbf{r}^n;\lambda)}}{\int \mathrm{d}\mathbf{r}^n \delta(\mathbf{R}^N - M_{r\to R}(\mathbf{r}^n)) e^{-\beta u(\mathbf{r}^n;\lambda)}} \right) \tag{B3}$$

and simplify using the integration by parts formulas used in ref 65 to obtain

$$\frac{\mathrm{d}\nabla_R U(\mathbf{R}^N;\lambda)}{\mathrm{d}\lambda} = \left\langle M^{\dagger}_{r\to R}\left(\frac{\mathrm{d}\nabla_r u(\mathbf{r}^n;\lambda)}{\mathrm{d}\lambda} \right) \right\rangle_{\mathbf{R}^N,\lambda} - \left\langle \frac{\mathrm{d}u(\mathbf{r}^n;\lambda)}{\mathrm{d}\lambda} M^{\dagger}_{r\to R}(\nabla_r \beta u(\mathbf{r}^n)) \right\rangle_{\mathbf{R}^N,\lambda} + \left\langle \frac{\mathrm{d}u(\mathbf{r}^n;\lambda)}{\mathrm{d}\lambda} \right\rangle_{\mathbf{R}^N,\lambda} \langle M^{\dagger}_{r\to R}(\nabla_r \beta u(\mathbf{r}^n)) \rangle_{\mathbf{R}^N,\lambda} \tag{B4}$$

Finally, rearrangement and grouping leads to eq 7, the transport-like SCI equation in the main text. This corresponds to the λ derivative of the g-YBG equations with a complete basis set.

■ ASSOCIATED CONTENT

Supporting Information

CG potentials and RDFs using the reference parametrization, complete sets of sensitivity comparisons, and complete sets of predicted potentials for both the methanol and sodium chloride systems as well as the complete set of RDFs comparing the predicted potentials to the actual RDF. The Supporting Information is available free of charge on the ACS Publications website at DOI: 10.1021/acs.jctc.5b00180.

■ AUTHOR INFORMATION

Corresponding Author

*Fax: 773-702-0805. Phone: 773-702-7250. E-mail: gavoth@uchicago.edu.

Author Contributions

‡J.W.W. and J.F.D. contributed equally to this work.

Notes

The authors declare no competing financial interest.

■ ACKNOWLEDGMENTS

This research was conducted with United States Government support under and awarded by the Department of Defense, High Performance Computing Modernization Project (HPCMP), under the National Defense Science and Engineering Graduate (NDSEG) Fellowship Program 32 CFR 168 a. Support was also provided by the Office of Naval Research under Grant N00014-13-1-0058. This work used the computing resources of the University of Chicago Research Computing Center.

■ REFERENCES

(1) Müller-Plathe, F. Coarse-Graining in Polymer Simulation: From the Atomistic to the Mesoscopic Scale and Back. *ChemPhysChem* **2002**, *3*, 754−769.

(2) Noid, W. G. Perspective: Coarse-Grained Models for Biomolecular Systems. *J. Chem. Phys.* **2013**, *139*, 090901.

(3) Brini, E.; Algaer, E. A.; Ganguly, P.; Li, C.; Rodriguez-Ropero, F.; van der Vegt, N. F. A. Systematic Coarse-Graining Methods for Soft Matter Simulations – A Review. *Soft Matter* **2013**, *9*, 2108−2119.

(4) Voth, G. A. *Coarse-Graining of Condensed Phase and Biomolecular Systems*; CRC Press: Boca Raton, 2009.

(5) Louis, A. A. Beware of Density Dependent Pair Potentials. *J. Phys.: Condens. Matter* **2002**, *14*, 9187−9206.

(6) Johnson, M. E.; Head-Gordon, T.; Louis, A. A. Representability Problems for Coarse-Grained Water Potentials. *J. Chem. Phys.* **2007**, *126*, 144509.

(7) Wong, C. F. Systematic Sensitivity Analyses in Free Energy Perturbation Calculations. *J. Am. Chem. Soc.* **1991**, *113*, 3208−3209.

(8) Wong, C. F.; Rabitz, H. Sensitivity Analyses and Principal Component Analysis in Free Energy Calculations. *J. Phys. Chem.* **1991**, *95*, 9628−9230.

(9) Rocklin, G. J.; Mobley, D. L.; Dill, K. A. Calculating the Sensitivity and Robustness of Binding Free Energy Calculations of Force Field Parameters. *J. Chem. Theory Comput.* **2013**, *9*, 3072−3083.

(10) Shirts, M. R.; Pande, V. S. Comparison of Efficiency and Bias of Free Energies Computed by Exponential Averaging, the Bennett Acceptance Ratio, and Thermodynamic Integration. *J. Chem. Phys.* **2005**, *122*, 144107.

(11) Paliwal, H.; Shirts, M. Using Multistate Reweighting to Rapidly and Effectively Explore Molecular Simulation Parameters Space for Nonbonded Interactions. *J. Chem. Theory Comput.* **2011**, *7*, 4115−4134.

(12) Shirts, M. R.; Chodera, J. D. Statistically Optimal Analysis of Samples from Multiple Equilibrium States. *J. Chem. Phys.* **2008**, *129*, 124105.

(13) Paliwal, H.; Shirts, M. R. Using Multistate Reweighting to Rapidly and Efficiently Explore Molecular Simulation Parameters Space for Nonbonded Interactions. *J. Chem. Theory Comput.* **2013**, *9*, 4700−4717.

(14) Fleischman, S. H.; Brooks, C. L. Thermodynamics of Aqueous Solvation: Solution Properties of Alcohols and Alkanes. *J. Chem. Phys.* **1987**, *87*, 3029−3037.

(15) Wong, C. F.; Thacher, T.; Rabitz, H., Sensitivity Analysis in Biomolecular Simulations. In *Reviews in Computational Chemistry*; Lipkowitz, K. B., Boyd, D. B., Eds.; Wiley & Sons: New York, 1998; Vol. *12*, pp 281−326.

(16) Cieplak, P.; Pearlman, D. A.; Kollman, P. A. Walking on the Free Energy Hypersurface of the 18-Crown-6 Ion System using Free Energy Derivatives. *J. Chem. Phys.* **1994**, *101*, 627−633.

(17) Zhu, S.-B.; Wong, C. F. Sensitivity Analysis of Water Thermodynamics. *J. Chem. Phys.* **1993**, *98*, 8892−8899.

(18) Wang, L.-P.; Head-Gordon, T.; Ponder, J. W.; Ren, P.; Chodera, J. D.; Eastman, P. K.; Martinez, T. J.; Pande, V. S. Systematic Improvement of a Classical Molecular Model of Water. *J. Phys. Chem. B* **2013**, *117*, 9956−9972.

(19) Krishna, V.; Noid, W. G.; Voth, G. A. The Multiscale Coarse-Graining Method. IV. Transferring Coarse-Grained Potentials Between Temperatures. *J. Chem. Phys.* **2009**, *131*, 024103.

(20) Izvekov, S.; Voth, G. A. A Multiscale Coarse-Graining Method for Biomolecular Systems. *J. Phys. Chem. B* **2005**, *109*, 2469−2473.

(21) Izvekov, S.; Voth, G. A. Multiscale Coarse Graining of Liquid-State Systems. *J. Chem. Phys.* **2005**, *123*, 134105.

(22) Noid, W. G.; Chu, J.-W.; Ayton, G. S.; Krishna, V.; Izvekov, S.; Voth, G. A.; Das, A.; Andersen, H. C. The Multiscale Coarse-Graining Method. I. A Rigorous Bridge Between Atomistic and Coarse-Grained models. *J. Chem. Phys.* **2008**, *128*, 244114.

(23) Noid, W. G.; Liu, P.; Wang, Y.; Chu, J.-W.; Ayton, G. S.; Izvekov, S.; Andersen, H. C.; Voth, G. A. The Multiscale Coarse-Graining Method. II. Numerical Implementation for Coarse-Grained Molecular Models. *J. Chem. Phys.* **2008**, *128*, 244115.

(24) Lu, L.; Voth, G. A. The Multiscale Coarse-Graining Method. VII. Free Energy Decomposition of Coarse-Grained Effective Potentials. *J. Chem. Phys.* **2011**, *134*, 224107.

DOI: 10.1021/acs.jctc.5b00180
J. Chem. Theory Comput. 2015, 11, 3547−3560

(25) Larini, L.; Lu, L.; Voth, G. A. The Multiscale Coarse-Graining Method. VI. Implementations of Three-Body Coarse-Grained Potentials. *J. Chem. Phys.* **2010**, *132*, 164107.
(26) Das, A.; Andersen, H. C. The Multiscale Coarse-Graining Method. IX. A General Method for Construction of Three Body Coarse-Grained Force Fields. *J. Chem. Phys.* **2012**, *136*, 194114.
(27) D'Adamo, G.; Pelissetto, A.; Pierleoni, C. Predicting the Thermodynamics by Using State-Dependent Interactions. *J. Chem. Phys.* **2013**, *138*, 234107.
(28) Qian, H.-J.; Carbone, P.; Chen, X.; Karimi-Varzaneh, H. A.; Liew, C. C.; Müller-Plathe, F. Temperature-Transferable Coarse-Grained Potentials for Ethylbenzene, Polystyrene, and Their Mixtures. *Macromolecules* **2008**, *41*, 9919−9929.
(29) Allen, E. C.; Rutledge, G. C. A Novel Algorithm for Creating Coarse-Grained, Density Dependent Implicit Solvent Models. *J. Chem. Phys.* **2008**, *128*, 154115.
(30) Allen, E. C.; Rutledge, G. C. Coarse-Grained Density Dependent Implicit Solvent Model Reliably Reproduces Model Surfactant System. *J. Chem. Phys.* **2009**, *130*, 204903.
(31) Izvekov, S.; Chung, P. W.; Rice, B. M. The Multiscale Coarse-Graining Method: Assessing Its Accuracy and Introducing Density Dependent Coarse-Grained Potentials. *J. Chem. Phys.* **2010**, *133*, 064109.
(32) Shen, J.-W.; Li, C.; van der Vegt, N. F. A.; Peter, C. Transferability of Coarse Grained Potentials: Implicit Solvent Models for Hydrated Ions. *J. Chem. Theory Comput.* **2011**, *7*, 1916−1927.
(33) Shell, M. S. The Relative Entropy is Fundamental to Multiscale and Inverse Thermodynamic Problems. *J. Chem. Phys.* **2008**, *129*, 144108.
(34) Murtola, T.; Falck, E.; Karttunen, M.; Vattulainen, I. Coarse-Grained Model for Phospholipid/Cholesterol Bilayer Employing Inverse Monte Carlo with Thermodynamic Constraints. *J. Chem. Phys.* **2007**, *126*, 075101.
(35) Lyubartsev, A. P.; Laaksonen, A. Calculation of Effective Interaction Potentials from Radial Distribution Functions: A Reverse Monte Carlo Approach. *Phys. Rev. E: Stat. Phys., Plasmas, Fluids, Relat. Interdiscip. Top.* **1995**, *52*, 3730−3737.
(36) Lu, L.; Voth, G. A., The Multiscale Coarse-Graining Method. In *Adv. Chem. Phys.*, Rice, S. A., Dinner, A. R., Eds.; Wiley-Interscience: New York, 2012; Vol. *149*.
(37) Noid, W. G.; Ayton, G. S.; Izvekov, S.; Voth, G. A., The Multiscale Coarse-Graining Method. In *Coarse-Graining of Condensed Phase and Biomolecular Systems*, Voth, G. A., Ed.; CRC Press: New York, 2008; pp 21−40.
(38) Mullinax, J. W.; Noid, W. G. Generalized Yvon-Born-Green Theory for Molecular Systems. *Phys. Rev. Lett.* **2009**, *103*, 198104.
(39) Mullinax, J. W.; Noid, W. G. A Generalized-Yvon-Born-Green Theory for Determining Coarse-Grained INteraction Potentials. *J. Phys. Chem. C* **2010**, *114*, 5661−5674.
(40) Reith, D.; Putz, M.; Müller-Plathe, F. Deriving Effective Mesoscale Potentials from Atomistic Simulations. *J. Comput. Chem.* **2003**, *24*, 1624−1636.
(41) Bilionis, I.; Zabaras, N. A Stochastic Optimization Approach to Coarse-Graining using a Relative Entropy Framework. *J. Chem. Phys.* **2013**, *138*, 044313.
(42) Chaimovich, A.; Shell, M. S. Coarse-Graining Errors and Numerical Optimization using a Relative Entropy Framework. *J. Chem. Phys.* **2011**, *134*, 094112.
(43) Rudzinski, J. F.; Noid, W. G. Coarse-Graining Entropy, Forces, and Structures. *J. Chem. Phys.* **2011**, *135*, 214101.
(44) Ercolessi, F.; Adams, J. B. Interatomic Potentials from First-Principles Calculations: The Force-Matching Method. *Europhys. Lett.* **1994**, *26*, 583−588.
(45) Lu, L.; Izvekov, S.; Das, A.; Andersen, H. C.; Voth, G. A. Efficient, Regularized, and Scalable Algorithms for Multiscale Coarse-Graining. *J. Chem. Theory Comput.* **2010**, *6*, 954−965.
(46) Plimpton, S. Fast Parallel Algorithms for Short-Range Molecular Dynamics. *J. Comput. Phys.* **1995**, *117*, 1−19.
(47) Brown, W. M.; Wang, P.; Plimpton, S. J.; Tharrington, A. N. Implementing Molecular Dynamics on Hybrid High Performance Computers - Short Range Forces. *Comput. Phys. Commun.* **2011**, *182*, 898−911.
(48) Brown, W. M.; Kohlmeyer, A.; Plimpton, S. J.; Tharrington, A. N. Implementing Molecular Dynamics on Hybrid High Performance Computers - Particle-Particle Particle-Mesh. *Comput. Phys. Commun.* **2012**, *183*, 449−459.
(49) Jorgensen, W. L.; Maxwell, D. S.; Tirado-Rives, J. Development and Testing of the OPLS All-Atom Force Field on Conformational Energetics and Properties of Organic Liquids. *J. Am. Chem. Soc.* **1996**, *118*, 11225−11236.
(50) Joung, I. S.; Cheatham, T. E. I. Molecular Dynamics Simulations of the Dynamic and Energetic Properties of Alkali and Halide Ions Using Water-Model-Specific Ion Parameters. *J. Phys. Chem. B* **2009**, *113*, 13279−13290.
(51) Jorgensen, W. L.; Chandrasekhar, J.; Madura, J. D.; Impey, R. W.; Klein, M. L. Comparison of Simple Potential Functions for Simulating Liquid Water. *J. Chem. Phys.* **1983**, *79*, 926−935.
(52) Cao, Z.; Dama, J. F.; Lu, L.; Voth, G. A. Solvent Free Ionic Solution Models for Multiscale Coarse-Graining. *J. Chem. Theory Comput.* **2013**, *9*, 172−178.
(53) Thorpe, I. F.; Goldenberg, D. P.; Voth, G. A. Exploration of Transferability in Multiscale Coarse-Grained Peptide Models. *J. Phys. Chem. B* **2011**, *115*, 11911−11926.
(54) Christ, C. D.; van Gunsteren, W. F. Enveloping Distribution Sampling: A Method to Calculate Free Energy Differences from a Single Simulation. *J. Chem. Phys.* **2007**, *126*, 184110.
(55) Efron, B. Nonparametric Estimates of Standard Error: The Jackknife, the Boostrap and Other Methods. *Biometrika* **1981**, *68*, 589−599.
(56) Jones, H. L. Jacknife Estimation of Functions of Stratum Means. *Biometrika* **1974**, *61*, 343−348.
(57) Cameron, A. C.; Gelbach, J. B.; Miller, D. L. Boostrap-Based Improvements for Inference with Clustered Errors. *Rev. Econ. Stat.* **2008**, *90*, 414−427.
(58) Wang, L.-P.; Chen, J.; Van Voorhis, T. Systematic Parameterization of Polarizable Force Fields from Quantum Chemistry Data. *J. Chem. Theory Comput.* **2013**, *9*, 452−460.
(59) Cho, H. M.; Chu, J.-W. Inversion of Radial Distribution Functions to Pair Forces by Solving the Yvon-Born-Green Equation Iteratively. *J. Chem. Phys.* **2009**, *131*, 134107.
(60) Lu, L.; Dama, J. F.; Voth, G. A. Fitting Coarse-Grained Distribution Functions through an Iterative Force-Matching Method. *J. Chem. Phys.* **2013**, *139*, 121906.
(61) Rudzinski, J. F.; Noid, W. G. Investigation of Coarse-Grained Mappings via an Iterative Generalized Yvon-Born-Green Method. *J. Phys. Chem. B* **2014**, *118*, 8295−8312.
(62) Molinero, V.; Moore, E. B. Water Modeled as an Intermediate Element between Carbon and Silicon. *J. Phys. Chem. B* **2009**, *113*, 4008−4016.
(63) Angell, C. A.; Bressel, R. D.; Hemmati, M.; Sare, E. J.; Tucker, J. C. Water and Its Anomalies in Perspective: Tetrahedral Liquids with and without Liquid-Liquid Phase Transitions. Invited Lecture. *Phys. Chem. Chem. Phys.* **2000**, *2*, 1559−11566.
(64) Singh, M.; Dhabal, D.; Nguyen, A. H.; Molinero, V.; Chakravarty, C. Triplet Correlations Dominate the Transition from Simple to Tetrahedral Liquids. *Phys. Rev. Lett.* **2014**, *112*, 147801.
(65) Dama, J. F.; Sinitskiy, A. V.; McCullagh, M.; Weare, J.; Roux, B.; Dinner, A. R.; Voth, G. A. The Theory of Ultra-Coarse-Graining. 1. General Principles. *J. Chem. Theory Comput.* **2013**, *9*, 2466−2480.

DOI: 10.1021/acs.jctc.5b00180
J. Chem. Theory Comput. 2015, 11, 3547−3560